Corty, C., and A. S. Foust, "Surface Variables in Nucleate Boiling," *AIChE Symposium Ser.*, No. 17, **51**, 1 (1955).
Coulson, J. M., and R. R. Mehta, "Heat Transfer Coefficients in a Climbing Film Evaporator," *Trans. Inst. Chem. Engrs.*, **31**, 208 (1953).
Day, J. A., "Production of Droplets and Salt Nuclei by the Bursting of Air-Bubble Films," *Quart. J. Royal Meteor. Soc.*, **90**, 72 (1964).
Dengler, C. E., and J. N. Addoms, "Heat Transfer Mechanism for Vaporization of Water in a Vertical Tube," *AIChE Symposium Ser.*, No. 18, **52**, 95 (1956).
Fletcher, Leroy S., Valentinas Sernas, and Lawrence S. Galowin, "Evaporation from Thin Water Films on Horizontal Tubes," *Ind. Eng. Chem. Process Design Develop.*, **13**, 265 (1974).
Gaertner, R. F., "Photographic Study of Nucleate Pool Boiling on a Horizontal Surface," *J. Heat Transfer*, **87C**, 17 (1965).
Hewitt, G. F., and N. S. Hall-Taylor, *Annular Two-Phase Flow*, p. 18, Pergamon Press, New York (1970).
Hospeti, N. B., and R. B. Mesler, "Vaporization at the Base of Bubbles of Different Shape During Nucleate Boiling of Water," *AIChE J.*, **15**, 214 (1969).
Howell, J. R., and Robert Siegel, "Incipience, Growth and Detachment of Boiling Bubbles in Saturated Water From Artificial Nucleation Sites of Know Geometry and Size," *Proc. 3rd International Heat Transfer Conference*, Vol. IV, p. 12, Am. Institute Chemical Engineers, New York (1966).
Iida, Yoshihiro, and Kiyosi Kobayasi, "Distributions of Void Fraction Above a Horizontal Heating Surface in Pool Boiling," *Bull. JSME*, **12**, 283 (1969).
Johnson, M. A., Jr., J. de la Peña, and R. B. Mesler, "Bubble Shapes in Nucleate Boiling," *AIChE J.*, **12**, 344 (1966).
Katto, Y., and M. Kunihiro, "Study of the Mechanism of Burn-Out in Boiling System of High Burn-Out Heat Flux," *Bull. JSME*, **16**, 1357 (1973).
Katto, Y., S. Yokoya, and M. Yasunaka, "Mechanism of Boiling Crisis and Transition Boiling in Pool Boiling," *Heat Transfer 1970*, Vol. V, B 3.2, Elsevier, New York (1970).
Kirby, D. B., "Boiling Near the Critical Heat Flux on Horizontal Plates," Ph.D. thesis, Univ. Ill., Urbana (1963).
———, and J. W. Westwater, "Bubble and Vapor Behavior on a Heated Horizontal Plate During Pool Boiling Near Burnout," *AIChE, Symposium Ser.*, No. 57, **61**, 238 (1965).
Kirshbaum, E., "New Data on Heat Transfer with and Without Change in State," *Chem. Eng. Technol.*, **24**, 393 (1952).
Kovács, Akos, and R. B. Mesler, "Making and Testing Small Surface Thermocouples for Fast Response," *Rev. Sci. Instr.*, **35**, 485 (1964).
Kusuda, H., and K. Nishikawa, "A Study of Nucleate Boiling in Liquid Film," *Mem. Faculty Engineering, Kyushu University*, **27**, 155 (1967).
Moissis, Raphael, and Paul Berenson, "On the Hydrodynamic Transitions in Nucleate Boiling," *J. Heat Transfer*, **85C**, 221 (1963).
Moore, F. D., and R. B. Mesler, "The Measurement of Rapid Surface Temperature Fluctuations During Nucleate Boiling of Water," *AIChE J.*, **7**, 620 (1961).
Newitt, D. M., N. Dombrowski, and F. H. Knelman, "Liquid Entrainment 1 The Mechanism of Drop Formation From Gas or Vapor Bubbles," *Trans. Inst. Chem. Engrs.*, **32**, 244 (1954).
Nishikawa, K., H. Kusada, K. Yamasaki, and K. Tanaka, "Nucleate Boiling at Low Liquid Levels," *Bull. JSME*, **10**, 328 (1967).
Norman, W. S., and V. McIntyre, "Heat Transfer to a Liquid Film on a Vertical Surface," *Trans. Inst. Chem. Engrs.*, **38**, 301 (1960).
Parizhskiy, O. V., V. P. Chepurnenko, L. F. Lagota, and L. F. Taranets, "Study of Boiling Heat Transfer with a Falling Film of Refrigerant," *Heat Transfer-Soviet Research*, **4**, 43 (1972).
Robinson, Donald B., and Donald L. Katz, "Effect of Vapor Agitation on Boiling Coefficients," *Chem. Engr. Progr.*, **47**, 317 (1951).
Rychkov, A. I., and V. K. Pospelov, "Heat Transfer During Film Evaporation of Caustic Soda Solutions," *Khim. Pro.*, **5**, 426 (1959) CE-TRANS-3944.
Sephton, Hugo H., "Interface Enhancement for Vertical Tube Evaporators," ASME Paper 71-HT-38 (1971).
Stock, Bernard, "Observations on Transition Boiling Heat Transfer Phenomena," Argonne National Laboratory, 6175 (1960).
Thomas, David G., and L. G. Alexander, "Improved High-Performance Fluted Tube for Thin-Film Evaporation and Condensation," *Desalination*, **8**, 13 (1970).
Thomas, David G., and Gale Young, "Thin-Film Evaporation Enhancement by Finned Surfaces," *Ind. Eng. Chem. Process Design Develop.*, **9**, 317 (1970).
Toda, Saburo, and Hideo Ushida, "Study of Liquid Film Cooling with Evaporation and Boiling," *Heat Transfer-Japanese Research*, **2**, 44 (1973).
Williams, D. D., and R. B. Mesler, "The Effect of Surface Orientation on Delay Time of Bubbles From Artificial Sites During Nucleate Boiling," *AIChE J.*, **13**, 1020 (1967).
Yatabe, J. M., and J. W. Westwater, "Bubble Growth Rates for Ethanol-Water and Ethanol-Isopropanol Mixtures," *Chem. Eng. Progr. Symposium Ser. No. 64*, **62**, 17 (1966).
Zuber, Novak, "Recent Trends in Boiling Heat Transfer Research Part I: Nucleate Pool Boiling," *Appl. Mechanics Rev.*, **17**, 663 (1964).

Manuscript received March 28, 1975; revision received October 9, and accepted October 10, 1975.

Surface Reaction with Combined Forced and Free Convection

The influence of combined forced and free convection on the surface reaction of a laminarly flowing species in a rectangular channel is studied. The free convective motion, which is superimposed upon the main axial flow, arises from a transverse density gradient produced by the release of a reaction product, or heat, at the channel wall. A numerical stream function-vorticity method is employed to solve the three-dimensional conservation equations in the case of large Schmidt number. Effects of aspect ratio, diffusivity ratio, surface reaction rate, and Rayleigh number upon the overall reactant conversion rate and local Sherwood number are examined. Reasonable agreement is obtained with experimental data for a hydrochloric acid-calcium carbonate surface reaction.

CHING-YUAN CHANG
JAMES A. GUIN
Department of Chemical Engineering
Auburn University
Auburn, Alabama 36830
and
LOY D. ROBERTS
Halliburton Services
Duncan, Oklahoma 73533

Correspondence concerning this paper should be addressed to James A. Guin.

SCOPE

In chemical kinetics investigations and in the design of reactors, the engineer must consider the fact that the overall reactant conversion rate may be influenced significantly by transport phenomena. Examples of diffusional influence upon reactions in laminar and turbulent flow are provided by Solbrig and Gidaspow (1967, 1968). Quite accurate estimates of transport effects are possible when the transport of reactant occurs solely by forced convection and molecular diffusion; however, if the system physical properties are such that reactant transport is influenced by both forced and free convective motions, then the combined net result cannot be predicted so accurately. Combined forced and free convection has been found by Roberts and Guin (1975) to be an important flow regime governing the conversion rate of acids used in oil well stimulation treatments, while a similar flow regime has been observed by Derzansky and Gill (1974) in reverse osmosis studies. The former situation is of practical importance in governing the penetration of acid into fractures in limestone and dolomite oil reservoirs. Besides mass transfer, heat transfer rates are sometimes controlled by combined forced and free convection as exemplified by the studies of Cheng et al. (1972) and Ou et al. (1974).

Each of the above investigations is concerned with the axial flow of fluid in a horizontal channel. Because of a particular process occurring at the channel wall, that is, heat transfer, mass transfer, or surface reaction, there arises a transverse concentration or temperature profile, which in turn gives rise to a density variation in the fluid. Since the channel is oriented horizontally, the action of gravity upon the variable density fluid induces a secondary circulation which is superimposed upon the main axial flow, yielding the so-called combined forced and free convective regime. This secondary flow influences the rate of transport to the channel wall, and the net result is a phenomenon wherein the conservation of momentum and mass or heat are intimately coupled. This complex interaction makes it difficult to predict from empirical correlations the performance of processes which operate in such a combined flow regime.

The objective of this study was to investigate the influence of the transport phenomena upon conversion of a chemical reactant in the combined flow regime. By analytical and numerical study, the governing parameters were identified, and the interaction of fluid mechanics with the surface reaction kinetics was studied. Proceeding in this manner allowed explanation and correlation of some earlier experimental results for surface reactions influenced by buoyancy forces, as well as providing a rough guide for ascertaining the importance of such phenomena in similar processes.

CONCLUSIONS AND SIGNIFICANCE

Analytical representation of surface reaction in the combined forced and free convection regime has shown the system to be governed by four dimensionless parameters, namely, aspect ratio, diffusivity ratio (Lewis number), surface reactivity (Damköhler number), and Rayleigh number. The effect of each parameter upon reactant conversion and local Sherwood number was determined numerically by using a finite-difference stream function-vorticity formulation, and the results were presented graphically. For $Ra > 10^3$, increases in the overall reaction rate as compared to the classical Graetz solution appeared between $z \sim 10^{-3}$ and 0.5. By using an estimated $Ra = 6.6 \times 10^6$, the theory was shown to satisfactorily account for the experimentally observed conversion rate of aqueous hydrochloric acid in a limestone channel. The graphical results presented herein may be used to predict the overall reactant conversion in processes where species transport is influenced by combined forced and free convection.

The overall rate of a chemical reaction process, particularly a fluid-solid reaction, is often times determined by a combination of intrinsic chemical kinetics and transport phenomena. Considerable success has been realized already in modeling surface reactions in rectilinear laminar flow, where the transport of chemical species occurs by molecular diffusion (Solbrig and Gidaspow, 1967; Lyczkowski et al., 1967), and in turbulent flow, where an empirical eddy diffusivity may be employed (Schechter and Wissler, 1962; Solbrig and Gidaspow, 1968). In these forced convection studies, the convective motions were the results of imposed pressure gradients and/or molecular diffusion fluxes, and the fluid properties were considered constant. At the other end of the spectrum, free convection with surface reaction has been studied recently wherein the convective motion arose solely from buoyancy forces caused by temperature induced density gradients (Gray and Kostin, 1974). In addition, numerous studies of transient free convection with various heat transfer boundary conditions have been made by Churchill and co-workers (Ozoe and Churchill, 1972; Ozoe et al., 1974).

This paper examines a flow regime intermediate between the two noted above, that of combined forced and free convection. The geometry considered is that of a horizontal rectangular duct in which a surface reaction occurs upon the two vertical sides, while the top and bottom walls are inert. This surface reaction is visualized as resulting in the release of heat, or a reaction product, which changes the local fluid density, thereby giving rise to a buoyancy induced free convective motion which becomes superimposed upon the main axial flow. The resulting three-dimensional velocity field thus partially controls the transport of reactant to the surface and thereby influences the overall reactant conversion rate. In the combined forced and free convection region, calculations have been made for several heat transfer boundary conditions by Cheng and co-workers (Cheng et al., 1972; Ou et al., 1974). The calculations performed here are similar except that two species equations must be considered, one for the reactant and one for the product (possibly heat) species.

MATHEMATICAL MODEL

Consider the horizontal rectangular duct shown in Figure 1, in which reactive species A experiences a first-order surface reaction given stoichiometrically by $\delta_a A = \delta_b B$ on the two vertical sides. The fluid density is dependent upon the concentration of product B, and hence a transverse density gradient perpendicular to the gravitational acceleration arises by virtue of the surface reaction. The duct is considered to have an inert inlet region, so

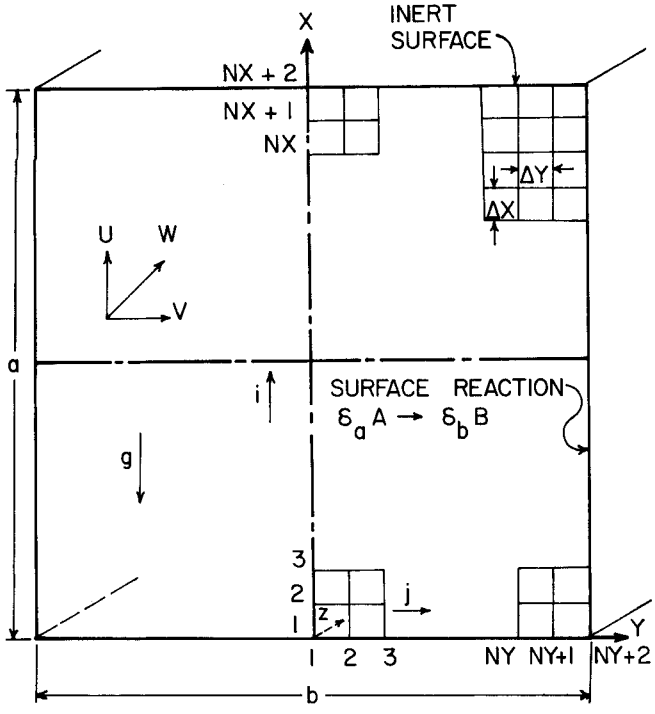

Fig. 1. Coordinate and grid system for surface reaction in a horizontal duct.

that the fluid enters the reactive section with a fully developed rectilinear laminar velocity profile. If all variations in fluid properties are ignored, except that of the density in the body force term, then the governing system equations are

$$\nabla \cdot \mathbf{V} = 0 \tag{1}$$

$$(\mathbf{V} \cdot \nabla)\mathbf{V} = \frac{-1}{\rho}\nabla P + \mathbf{g} + \nu\nabla^2\mathbf{V} \tag{2}$$

$$\mathbf{V} \cdot \nabla C_i = D_i \nabla^2 C_i, \; i = A, B \tag{3}$$

The applicable boundary conditions for Equations (1), (2), and (3) are

$$U = V = W = 0 \text{ on all walls} \tag{4}$$

$$U = V = 0 \text{ at } Z = 0 \tag{5}$$

$$W = W_o(X, Y) \text{ at } Z = 0 \tag{6}$$

$$\frac{\partial C_A}{\partial n} = \frac{\partial C_B}{\partial n} = 0 \text{ at } X = 0, a \text{ and } Y = 0 \tag{7}$$

$$-D_A \frac{\partial C_A}{\partial Y} = \frac{\delta_a D_B}{\delta_b} \cdot \frac{\partial C_B}{\partial Y} = kC_A \text{ at } Y = \pm b/2 \tag{8}$$

In further accord with the Boussinesq approximation, the density variation is represented by

$$\frac{\rho}{\rho_o} = 1 - \beta(C_B - C_{Bo}) \tag{9}$$

Equations (1) to (9) also provide a mathematical description of the analogous heat transfer phenomenon occurring when component A reacts at an adiabatic surface with heat of reaction ΔH. In this case, component B becomes heat rather than matter, and if one equates $C_B \equiv T$, $D_B \equiv \alpha$, and $\delta_b \equiv -\Delta H/\rho C_p$, then the mathematical representation of the two physical processes becomes identical. For this to be valid, of course, the surface rate constant k can not be a function of T. Thus, the density variation giving rise to the secondary flow may be visualized as arising from either a temperature or a concentration gradient.

If we define p_o and W_o as the pressure and velocity in steady, rectilinear, laminar flow, then these two quantities satisfy the respective equations

$$\frac{1}{\rho_o}\frac{\partial p_o}{\partial X} + g_x = 0 \tag{10}$$

$$-\frac{1}{\rho_o}\frac{\partial p_o}{\partial Z} + \nu\left(\frac{\partial^2 W_o}{\partial Y^2} + \frac{\partial^2 W_o}{\partial X^2}\right) = 0 \tag{11}$$

Introducing the perturbation quantities p' and W' by $p = p_o + p'$ and $W = W_o + W'$ and writing (1) to (3) and (11) in dimensionless component form, we get

$$\frac{\partial u}{\partial x} + \frac{\partial v}{\partial y} + \frac{\partial w'}{\partial z} = 0 \tag{12}$$

$$\frac{1}{Sc}\left[u\frac{\partial u}{\partial x} + v\frac{\partial u}{\partial y} + (w_o + w')\frac{\partial u}{\partial z}\right] = -\frac{\partial p'^*}{\partial x} + \nabla^2 u + \frac{1}{Pe^2}\frac{\partial^2 u}{\partial z^2} + Ra\theta_B \tag{13}$$

$$\frac{1}{Sc}\left[u\frac{\partial v}{\partial x} + v\frac{\partial v}{\partial y} + (w_o + w')\frac{\partial v}{\partial z}\right] = -\frac{\partial p'^*}{\partial y} + \nabla^2 v + \frac{1}{Pe^2}\frac{\partial^2 v}{\partial z^2} \tag{14}$$

$$\frac{1}{Sc}\left[u\frac{\partial}{\partial x}(w_o + w') + v\frac{\partial}{\partial y}(w_o + w') + (w_o + w')\frac{\partial w'}{\partial z}\right] = -\frac{1}{Pe^2}\frac{\partial p'^*}{\partial z} + \nabla^2 w' + \frac{1}{Pe^2}\frac{\partial^2 w'}{\partial z^2} \tag{15}$$

$$u\frac{\partial \theta_A}{\partial x} + v\frac{\partial \theta_A}{\partial y} + (w_o + w')\frac{\partial \theta_A}{\partial z} = \nabla^2\theta_A + \frac{1}{Pe^2}\frac{\partial^2 \theta_A}{\partial z^2} \tag{16}$$

$$\frac{1}{D^*}\left[u\frac{\partial \theta_B}{\partial x} + v\frac{\partial \theta_B}{\partial y} + (w_o + w')\frac{\partial \theta_B}{\partial z}\right] = \nabla^2\theta_B + \frac{1}{Pe^2}\frac{\partial^2 \theta_B}{\partial z^2} \tag{17}$$

$$\nabla^2 w_o = \frac{1}{\nu\rho_o}\frac{De}{\overline{W}_o Pe}\frac{\partial P_o}{\partial z} \tag{18}$$

where the Laplacian retains only the x and y dependence. Equations (12) to (18) will now be greatly simplified by neglecting the terms divided by Pe^2 and Sc, thus yielding an approximate set of equations valid for large Pe and Sc numbers. Some idea as to the range of validity of this approximation may be obtained from the literature. Calculations performed by Ozoe and Churchill (1972) and by Elder (1966) indicate that the inertia terms have very little effect in problems of this type for $Sc > 10$ and hence that $Sc \rightarrow \infty$ yields a reasonable approximation in most instances. In the same light, research on the Graetz problem by Sorensen and Stewart (1974) and others has shown that for Pe greater than about 40, the axial diffusion terms are negligible, and hence $Pe \rightarrow \infty$ is an allowable simplification. After neglecting the terms

for $Pe \to \infty$ and $Sc \to \infty$, one may conclude from (15) and (4) that $w' = 0$ everywhere. This major simplification allows (12) to (14) to be cast in a stream function—vorticity framework, namely

$$\nabla^2\zeta = Ra\partial\theta_B/\partial y \tag{19}$$

$$\nabla^2\Psi = \zeta \tag{20}$$

$$\nabla^2\theta_A = u\frac{\partial\theta_A}{\partial x} + v\frac{\partial\theta_A}{\partial y} + w_o\frac{\partial\theta_A}{\partial z} \tag{21}$$

$$\nabla^2\theta_B = \frac{1}{D^*}\left(u\frac{\partial\theta_B}{\partial x} + v\frac{\partial\theta_B}{\partial y} + w_o\frac{\partial\theta_B}{\partial z}\right) \tag{22}$$

$$\nabla^2 w_o = -c \tag{23}$$

The solution to (19) to (23) must satisfy the following boundary and symmetry conditions:

$$\theta_A = 1 \text{ and } u = v = \theta_B = 0 \text{ at } z = 0 \tag{24}$$

$$w_o = \Psi = 0 \text{ on all walls} \tag{25}$$

$$\frac{\partial w_o}{\partial y} = \Psi = \zeta = 0 \text{ along } y = 0 \tag{26}$$

$$\zeta = \frac{\partial^2\Psi}{\partial n^2} \text{ on all walls} \tag{27}$$

$$\frac{\partial\theta_A}{\partial n} = \frac{\partial\theta_B}{\partial n} = 0 \text{ along } y = 0 \text{ and } x = 0, \frac{\gamma+1}{2\gamma} \tag{28}$$

$$-\frac{\partial\theta_A}{\partial y} = D^*\frac{\partial\theta_B}{\partial y} = P\theta_A \text{ along } y = \pm\frac{\gamma+1}{4} \tag{29}$$

From (19) to (29), it is concluded that the reactant concentration θ_A will have the dependence $\theta_A = \theta_A(x, y, z, Ra, \gamma, P, D^*)$.

QUANTITIES OF INTEREST

Several quantities of engineering importance may be obtained from the solution to the model formulated by (19) to (29). The bulk mean concentration for the reactant is

$$\bar{\theta}_A = \int_A w_o\,\theta_A\,dA \Big/ \int_A w_o\,dA \tag{30}$$

while the local Sherwood number is

$$Sh = \frac{\overline{\left.\frac{\partial\theta_A}{\partial y}\right|_{y=\frac{\gamma+1}{4}}}}{\left[\bar{\theta}_A\left(x, \frac{\gamma+1}{4}\right) - \bar{\theta}_A\right]} \tag{31}$$

In (31), the overbars on wall-evaluated quantities indicate averages over the reactive perimeter. An alternative expression for Sh may be obtained through integration of (21) over the area A followed by an application of Green's theorem to yield

$$Sh = \frac{(1+\gamma)\frac{\partial\bar{\theta}_A}{\partial z}}{4\left[\bar{\theta}_A\left(x, \frac{\gamma+1}{4}\right) - \bar{\theta}_A\right]} \tag{32}$$

An average Sherwood number may be defined in the usual manner as

$$\overline{Sh} = \frac{1}{z}\int_o^z Sh\,dz \tag{33}$$

For the particular limiting case of the diffusion controlled reaction ($P \to \infty$), one has the overall material balance relation

$$\bar{\theta}_A = \exp\left[\frac{-4}{1+\gamma}\overline{Sh}\,z\right] \tag{34}$$

which is useful for checking the precision and consistency of numerical results. Equations analogous to (30) to (34) may be obtained for component B in a similar manner.

SOLUTION OF MODEL EQUATIONS

Since the primary interest here was on elucidating physical behavior, certain known finite-difference methods were employed to effect the solution. To set up the finite-difference formulation, a system of grid points was established as shown in Figure 1. Because of axisymmetry, only half of the channel was considered. Since all quantities were known at the beginning of the reactive section, a simple explicit method with forward differences used was chosen for the solution of Equations (21) and (22). This technique, described as method V by Torrance (1968), has desirable conservation properties with respect to the convective terms between all points in the finite-difference grid. Stability is insured by choosing an appropriate three-point noncentral difference expression for the nonlinear x and y derivatives based upon the signs of u and v at each grid point.

The model requires the solution of the stream function-vorticity equations at each axial position. The ADI method was used to perform this calculation by introducing fictitious unsteady terms into (19) and (20). After each fictitious time step in the ADI solution, new wall vorticities were extrapolated from the interior stream function field by using a third-order Taylor expansion. The fact that wall vorticities were one time step behind the interior values became negligible as the steady state was approached. Once the steady stream function-vorticity fields were found, secondary velocity components were obtained by second-order central differences. The ADI method was also employed to solve (23) at the beginning of a calculation.

At any axial position, the interior concentration fields were found from the previously known field values and secondary velocity components at the prior axial location. Following this, the boundary concentration values at the new location were obtained by extrapolation from the interior values by using a second-order Taylor expansion. Of course, this calculation also results in a value for the local Sherwood number at the wall according to (31) and, as noted by Ozoe and Churchill (1972), is perhaps the least accurate feature of the entire computational procedure. Fortunately, an alternative Sherwood number may be found from (32), and comparison of the two values at each axial location yields some indication of the accuracy. Determination of the boundary concentration values then allows calculation of the secondary velocity components from (19) and (20), after which another axial step may be taken.

ACCURACY AND COMPUTATIONAL TIME

Several tests were performed to assess the accuracy of numerical solutions. The ADI solution of (19) to (20) with 150 grid points used checked within 1.5% of the analytical result in Timoshenko (1959). For $Ra = 3 \times 10^4$, a comparison of Sh computed with a 9×17 grid gave agreement to within about 3% of Cheng et al. (1972), while for $Ra = 0$, the numerical asymptotic Sh

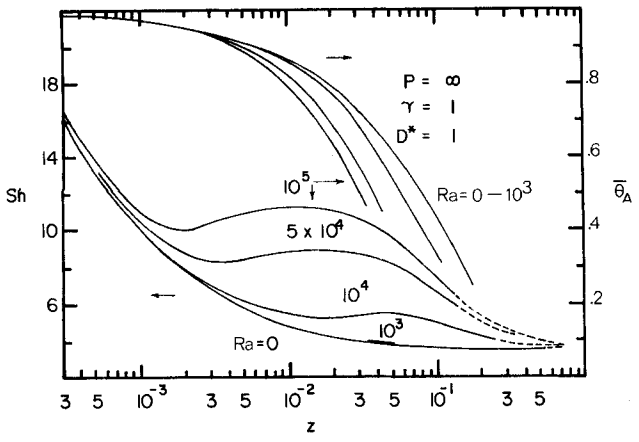

Fig. 2. Effect of Rayleigh number on bulk reactant concentration profile and local Sherwood number for diffusion controlled reaction in a square duct.

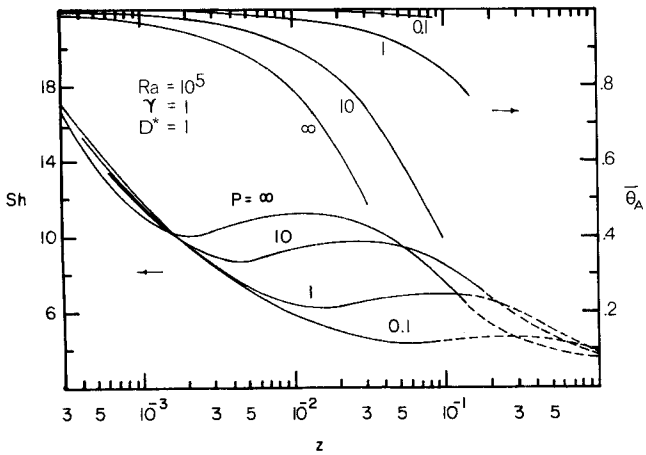

Fig. 3. Effect of surface reaction rate on bulk reactant concentration profile and local Sherwood number in a square duct.

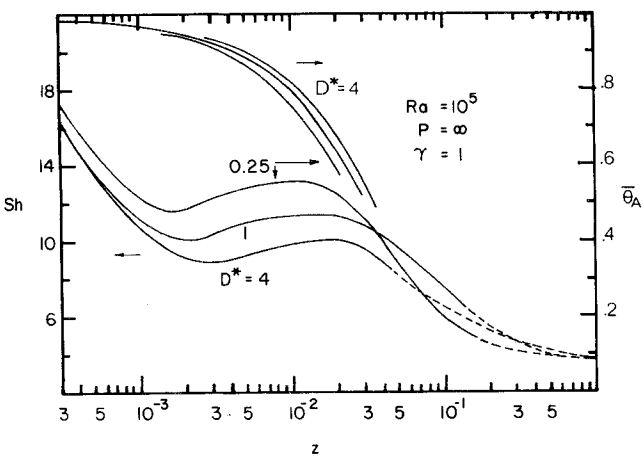

Fig. 4. Effect of diffusivity ratio on reactant bulk concentration profile and local Sherwood number for diffusion controlled reaction in a square duct.

was 3.06 vs. the analytical 3.091. Further comparisons, including Ou et al. (1974), and a study of grid size are given by Chang (1975). Complete solution of (19) to (23) with the usual 11 × 15 grid required about 1 hr. on an IBM 370/155.

RAYLEIGH NUMBER

The axial variation of mean reactant concentration and local Sherwood number for the diffusion controlled case in a square duct is shown in Figure 2 for various Rayleigh numbers. For $Ra > 10^3$, significant increases in overall

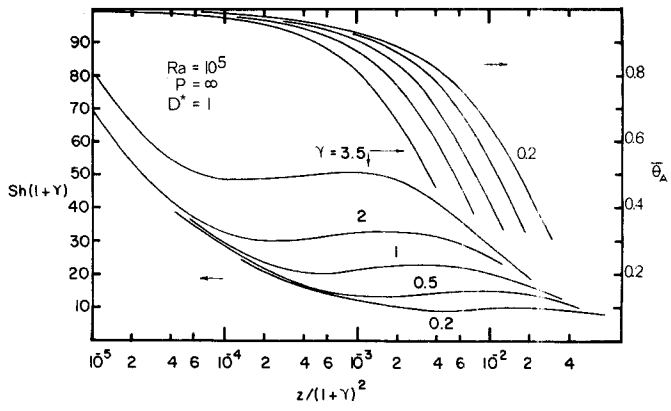

Fig. 5. Effect of aspect ratio on reactant bulk concentration profile and local Sherwood number for diffusion controlled reaction in a square duct. ($NX = 13$, $NY = 19$ for $\gamma = 2, 3.5$.)

reaction rates are caused by the secondary flow in the range between $z \sim 10^{-3}$ and 0.5, and the solutions depart from the constant properties curve, with higher Rayleigh numbers yielding increased reaction, as expected. For z greater than about 0.5, all Sh's approach the same asymptotic (Graetz) limit. The Sh's in Figure 2 have thus been extrapolated to the asymptotic value of 3.65 found numerically.

Of some practical importance when these results are used is the fact that $Sc \sim 10^3$ for liquids vs. ~ 1 for gases; therefore, for the same Re and channel geometry, z will be smaller for liquids than for gases. Thus, liquid phase applications will tend toward the entrance region, while gas phase applications may well lie nearer the fully developed region. The Sc number difference for liquids vs. gases is of further importance in that $Ra = Sc \cdot Gr$.

SURFACE REACTION RATE

Figure 3 shows Sh and $\overline{\theta}_A$ for $Ra = 10^5$ with various first-order reaction rate parameters. The crossover of the Sh at $z \sim 1.5 \times 10^{-3}$ is interesting. This net effect results from a combination of two phenomena. A higher value of P gives a thicker concentration boundary layer and lower values of Sh near the channel entrance; however, the higher values of P also result in greater secondary flow further downstream, giving rise to larger values of Sh and the resulting crossover. For comparison, the values of Sh with $Ra = 0$ were also computed (Chang, 1975). There was, of course, no crossover, and the values of Sh were everywhere greater at lower values of P. For $Ra = 0$, each Sh approached a different asymptotic value, depending upon P, and the curves in Figure 3 have been extrapolated to these values.

DIFFUSIVITY RATIO

Figure 4 presents the effect of diffusivity ratio upon Sh and $\overline{\theta}_A$. Again, there is an interesting crossover effect, which is absent when $Ra = 0$. A larger value of D^* reduces the transverse concentration gradient of component B and hence the secondary flow intensity. From Figure 4, it is seen that most of the reaction for $D^* = 0.25$ occurs much more rapidly and with greater intensity over a shorter region of the channel, than that for $D^* = 1.0$. This intense secondary flow, however, is self-defeating in a sense because being a mixing mechanism, it destroys the very concentration gradient causing it, thus resulting in the sharper maximum in Sh for $D^* = 0.25$ as compared to $D^* = 1.0$.

ASPECT RATIO

The effects of aspect ratio upon $\overline{\theta}_A$ and Sh are shown in Figure 5 for the diffusion controlled reaction with Ra

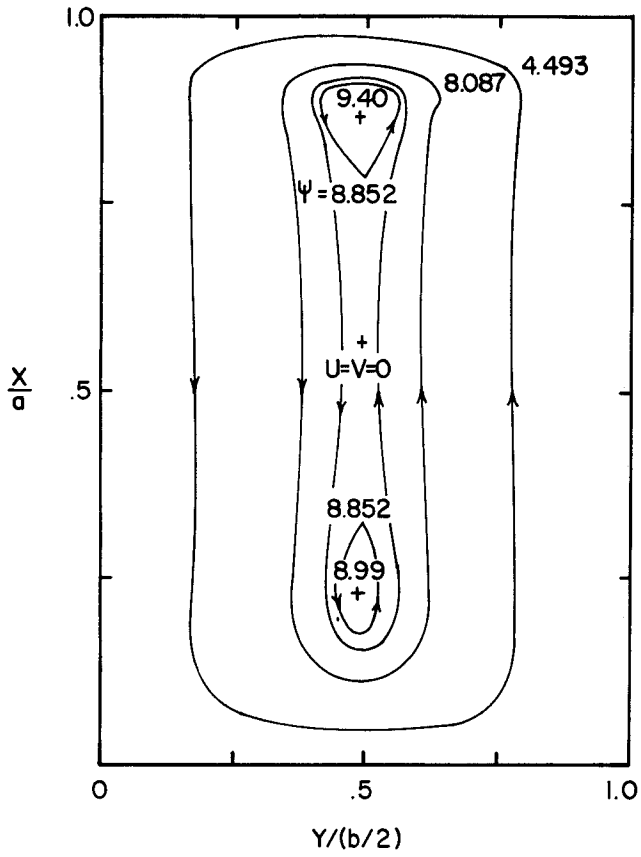

Fig. 6. Secondary flow streamlines at $z = 0.2117 \times 10^{-2}$ for $\gamma = 0.2$, $Ra = 10^5$, $P \rightarrow \infty$ and $D^* = 1$. ($NX = 27$, $NY = 19$.)

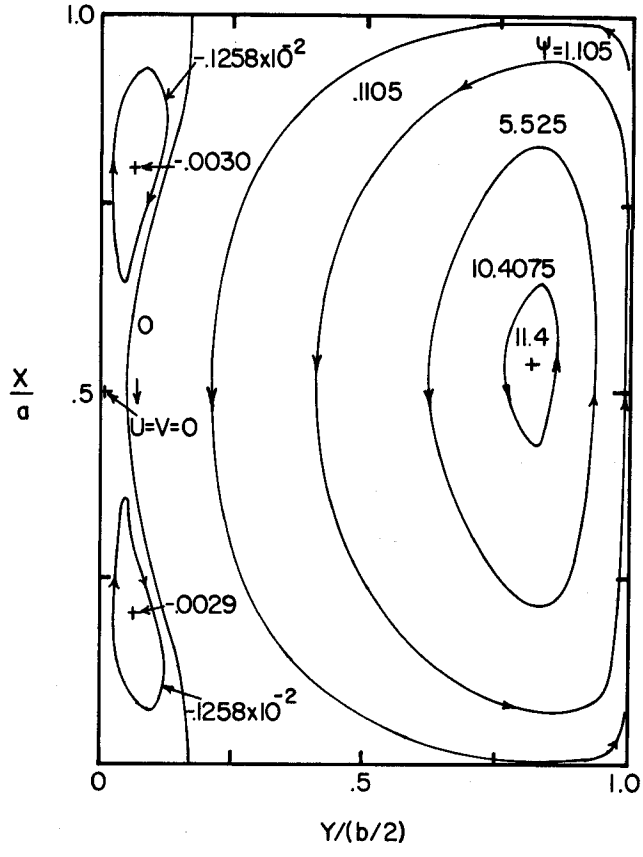

Fig. 7. Secondary flow streamlines at $z = 0.1062 \times 10^{-2}$ for $\gamma = 3.5$, $Ra = 10^5$, $P \rightarrow \infty$, and $D^* = 1$. ($NX = 13$, $NY = 19$.)

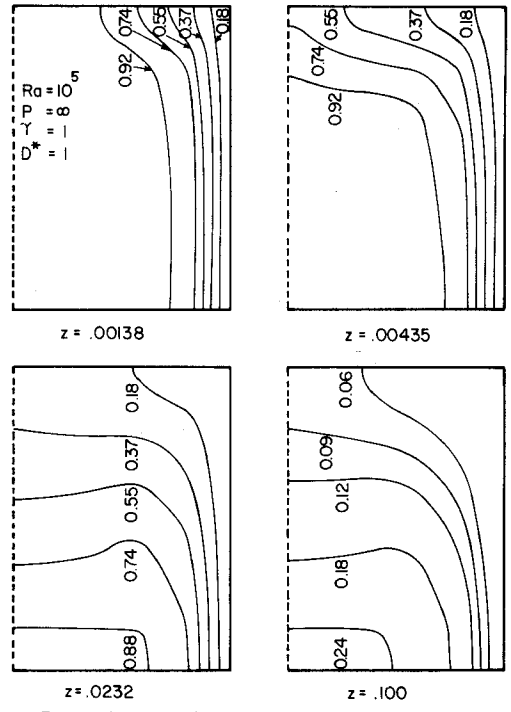

Fig. 8. Contour plots of reactant concentration.

$= 10^5$. The effects of secondary flow are more pronounced in the case of the short wide channel, while becoming virtually insignificant for small aspect ratio. From Figure 5 it is seen that the Sherwood number and hence secondary flow intensity reaches a maximum at lesser values of z for higher aspect ratios.

Several interesting secondary flow patterns have been observed numerically depending upon the aspect ratio. Examination of the streamlines for several aspect ratios, $Ra = 10^5$ and $P \rightarrow \infty$, revealed that in the entire channel cross section:

1. Two secondary flow vortices were present at all z for $\gamma = 1$ (square channel). 2. Four vortices were present from $z = 0.9651 \times 10^{-4}$ to 0.3986×10^{-2} for $\gamma = 0.2$ and from $z = 0.1045 \times 10^{-3}$ to 0.9198×10^{-3} for $\gamma = 0.5$. 3. Six vortices were present from $z = 0.8450 \times 10^{-4}$ to 0.2292×10^{-2} for $\gamma = 3.5$.

Typical streamlines for $\gamma = 0.2$ and 3.5 are presented in Figures 6 and 7 as an illustration of the secondary flow patterns. Figure 6 illustrates the secondary flow in a tall narrow channel. The less dense fluid near the right wall moves upward, while the more dense fluid near the center moves downward. Two vortices appear near the top and bottom walls and grow toward each other, eventually becoming one further downstream around $z = 0.4874 \times 10^{-2}$. For the short wide channel shown in Figure 7, the less dense fluid at the right-hand wall moves upward forcing the more dense adjacent fluid to move downward. The fluid near the center line, which for this aspect ratio is far away from the reactive wall, is almost stagnant, although it does move slightly in the opposite direction. Thus, two small vortices in addition to the larger usual one arise at the top and bottom corners near the center line. Proceeding downstream, these two vortices disappear as the dominant one grows. In the case of a square duct, only a single vortex is present.

Typical contour plots for reactant concentration are presented in Figure 8. Near the channel inlet, the contours are nearly vertical, indicating low secondary motion contribution to reactant transport, while further downstream the effect of secondary circulation is obvious. The most concentrated reactant remains near the lower center

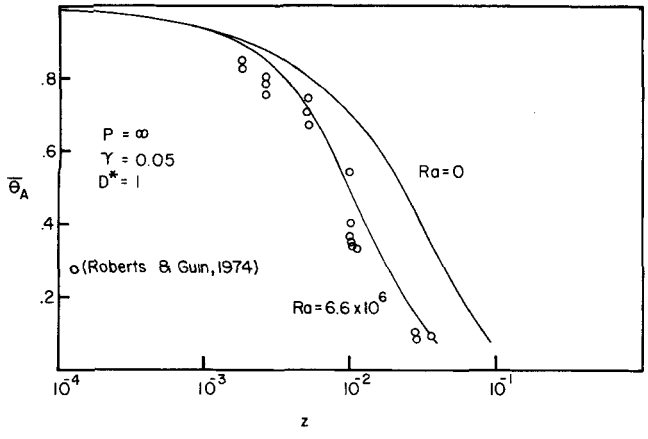

Fig. 9. Comparison of theory with experiment for reaction of hydrochloric acid in limestone channel. ($NX = 27$, $NY = 9$.)

of the channel, since it is more dense than the product being released at the vertical surface. Far downstream, the concentration contours would again become near vertical as the secondary flow diminishes and molecular diffusion again becomes the predominant transport mechanism.

COMPARISON WITH EXPERIMENT

Surface reaction experiments in the combined flow regime have been performed by Roberts and Guin (1974) who studied the surface reaction of hydrochloric acid in a rectangular duct with limestone walls. The overall stoichiometry of the reaction studied was

$$2HCl_{(aq)} + CaCO_{3(s)} \rightarrow CO_{2(aq)} + CaCl_{2(aq)} + H_2O \tag{35}$$

The surface kinetics of this system have been studied thoroughly by Lund et al. (1975) using the rotating disk geometry. At the conditions employed in the experiments of Roberts and Guin, the carbon dioxide remained in solution, and the surface reaction was essentially instantaneous and irreversible. If the fluid density is considered to be a function primarily of the calcium chloride concentration, and if the complexities of electrochemical ionic diffusion are represented approximately by a constant effective diffusivity (Roberts and Guin, 1975), then these experiments may be analyzed within the framework of the model developed here. By using the values $\beta = -80.9$ cm^3/g mole $CaCl_2$, $\delta_a/\delta_b = 2$ moles HCl/mole $CaCl_2$, $De = 0.385$ cm, $D_A = 4 \times 10^{-5}$ cm^2/s, $\nu = 0.012$ cm^2/s, $C_{Ao} = 0.0014$ g mole HCl/cm^3, the Rayleigh number may be estimated as -6.6×10^6. A comparison between the model prediction and the experimental data is presented in Figure 9. Secondary flow causes the data points to lie below the curve for $Ra = 0$; however, agreement with the solution for $Ra = 6.6 \times 10^6$ is reasonable. This comparison is encouraging; however, it would be desirable to perform additional experiments by using a system having more accurately defined parameters which adhere more closely to the assumptions made in the model formulation.

The reaction shown in (35) is exothermic, and one might expect a contribution to free convection from the density variation with temperature. As noted earlier, this heat release problem may also be analyzed within the framework presented here by simply renaming certain variables. Use of an approximate heat of reaction of -8.3 kcal/g mole and expansion coefficient of 1.5×10^{-4}/°C gives $Ra = 1.2 \times 10^5$ for this nonisothermal reaction problem. Further, the Lewis number (D^*) is estimated to be ~30. A computer run with these parameters yielded a curve negligibly different from that for $Ra = 0$ in Figure 9, showing that temperature variations would not cause significant free convection effects in the experiments of Roberts and Guin (1974), shown in Figure 9. The large value of D^* reduces the transverse density gradients in this case, thus minimizing free convective effects.

ACKNOWLEDGMENT

J. A. Guin and C. Y. Chang were partly supported by NSF Grant GK-37460. J. A. Guin also expresses grateful appreciation to Halliburton Services for support of this work.

NOTATION

a, b = height, width of rectangular channel
c = $-(\partial p_o/\partial z)(De/\nu\rho_o \overline{W}_o Pe)$, a constant
C = molar concentration
C_p = heat capacity
D = diffusivity
D^* = diffusivity ratio, D_B/D_A or Lewis number, α/D_A
De = equivalent diameter, $2ab/a + b$
g_x = gravitational acceleration
Gr = $\beta g_x De^3 \theta_c/\nu^2$
ΔH = heat of reaction
k = surface reaction rate constant
k_L = mass transfer coefficient
NX, NY = number of interior grid lines in x direction, y direction
n = coordinate normal to wall
P = reaction rate parameter, kDe/D_A
Pe = Peclet number, $ScRe$
Pr = Prandtl number, ν/α
p = pressure
p'^* = dimensionless pressure perturbation, $p'De^2/\rho_o\nu D_A$
Ra = Rayleigh number, $\beta g_x De^3 \theta_c/\nu D_A$
Re = Reynolds number, $\overline{W}_o De/\nu$
Sc = Schmidt number, ν/D_A
Sh = Sherwood number, $\overline{k}_L De/D_A$
T = temperature
U, V, W = velocity components in x, y, z directions
u, v = dimensionless velocities, DeU/D_A, DeV/D_A
w = dimensionless velocity, $W/\overline{W}_o$
X, Y, Z = rectangular coordinates
x, y = dimensionless coordinates, X/De, Y/De
z = dimensionless axial distance, $Z/DeScRe$

Greek Letters

α = thermal diffusivity
β = volume expansion coefficient [Equation (9)]
γ = aspect ratio, b/a
δ_a, δ_b = stoichiometric coefficients of A, B, respectively
θ_A = dimensionless concentration of A, C_A/C_{Ao}
θ_B = dimensionless concentration of B, $(C_B - C_{Bo})/\theta_c$
θ_c = $C_{Ao}/(\delta_a/\delta_b)$
ν = kinematic viscosity, μ/ρ
ζ = dimensionless vorticity, $\zeta = -\partial u/\partial y + \partial v/\partial x$
ρ = density
Ψ = dimensionless stream function, $u = -\partial\Psi/\partial y$ and $v = \partial\Psi/\partial x$

Superscripts

* = dimensionless variable
$\overline{\ }$ = average value
$'$ = perturbation quantity

Subscripts

A, B = species A, B
o = inlet value at $z = 0$ or value in rectilinear flow
w = wall evaluated quantity

LITERATURE CITED

Chang, C. Y., "Surface Reaction with Combined Forced and Free Convection," M.S. thesis, Auburn University, Ala. (1975).

Cheng, K. C., S. W. Hong, and G. J. Hwang, "Buoyancy Effects on Laminar Heat Transfer in the Thermal Entrance Region of Horizontal Rectangular Channels with Uniform Wall Heat Flux for Large Prandtl Number Fluids," *Intern. J. Heat Mass Transfer*, **15**, 1819 (1972).

Derzansky, L. J., and W. N. Gill, "Mechanisms of Brine-Side Mass Transfer in a Horizontal Reverse Osmosis Tubular Membrane," *AIChE J.*, **20**, 751 (1974).

Elder, J. W., "Numerical Experiments with Free Convection in a Vertical Slot," *J. Fluid Mech.*, **24**, 823 (1966).

Gray, W. G., and M. D. Kostin, "Natural Convection, Diffusion and Chemical Reaction in a Catalytic Reactor," *Chem. Eng. J.*, **8**, 1 (1974).

Lund, K., H. S. Fogler, C. C. McCune, and J. W. Ault, "Acidization—II. The Dissolution of Calcite in Hydrochloric Acid," *Chem. Eng. Sci.*, **30**, 825 (1975).

Lyczkowski, R. W., D. Gidaspow, and C. W. Solbrig, "Simultaneous Convective Diffusion of Reactants, Products, and Heat with a Surface Reaction," *AIChE Symposium Ser.*, No. 77, **63**, 1 (1967).

Ou, J. W., K. C. Cheng, and R. C. Lin, "Natural Convection Effects on the Graetz Problem in Horizontal Rectangular Channels with Uniform Wall Temperature for Large Pr," *Intern. J. Heat Mass Transfer*, **17**, 835 (1974).

Ozoe, H., and S. M. Churchill, "Hydrodynamic Stability and Natural Convection in Ostwald-de-Waele and Ellis Fluids: The Development of a Numerical Solution," *AIChE J.*, **18**, 1196 (1972).

Ozoe, H., K. Yamamoto, H. Sayama, and S. W. Churchill "Natural Convection in an Inclined Rectangular Channel Heated on One Side and Cooled on the Opposing Side," *Intern. J. Heat Mass Transfer*, **17**, 1209 (1974).

Roberts, L. D., and J. A. Guin, "Effects of Surface Kinetics in Fracture Acidizing," *Soc. Petrol. Eng. J.*, **14**, 385 (1974).

Roberts, L. D., and J. A. Guin, "A New Method for Predicting Acid Penetration Distance," *ibid.*, **15**, 277 (1975).

Schechter, R. S., and E. H. Wissler, "Turbulent Flow of Gas Through a Tube with Chemical Reaction at the Wall," *Chem. Eng. Sci.*, **17**, 937 (1962).

Solbrig, C. W., and Dimitri Gidaspow, "Convective Diffusion in a Rectangular Duct with One Catalytic Wall," *AIChE J.*, **13**, 346 (1967).

———, "Turbulent Mass Transfer with Arbitrary Order Surface Reaction in a Flat Duct," *Intern. J. Heat Mass Transfer*, **11**, 155 (1968).

Sorensen, J. P., and W. E. Stewart, "Computation of Forced Convection in Slow Flow Through Ducts and Packed Beds I. Extensions of the Graetz Problem," *Chem. Eng. Sci.*, **29**, 811 (1974).

Timoshenko, S., *Theory of Plates and Shells*, p. 180, McGraw-Hill, New York (1959).

Torrance, K. E., "Comparison of Finite-Difference Computations of Natural Convection," *J. Research Natl. Bur. Standards*, **72B**, 281 (1968).

Manuscript received April 15; revision received October 2, and accepted October 6, 1975.

A Theoretical Study of Pressure Drop for Non-Newtonian Creeping Flow Past an Assemblage of Spheres

A combination of Happel's free surface model and variational principles is used to obtain bounds on the drag offered by the creeping flow of a power law fluid past an assemblage of solid spheres. The theoretical predictions of the product of the Fanning friction factor f and Reynolds number Re_p are in close agreement with available experimental data on non-Newtonian flow through porous media. The product ($f\ Re_p$) reduces for the Newtonian case to that of Happel and Brenner.

V. MOHAN

and

J. RAGHURAMAN

Department of Chemical Engineering
Indian Institute of Technology
Madras 600 036, India

SCOPE

The flow of a Newtonian fluid through packed and fluidized beds has received considerable attention in the chemical engineering literature. A free surface model developed by Happel is widely used to predict the friction factor for Newtonian fluids. However, the analogous problem of flow of a non-Newtonian fluid through packed and fluidized beds has not been analyzed so far with this model. This paper extends the Happel's free surface model to the flow of power law fluids by making use of variational principles and presents an analysis for the friction factor in packed and fluidized beds.

CONCLUSIONS AND SIGNIFICANCE

A combination of Happel's free surface model and variational principles yields numerical values for the product of the Fanning friction factor f and the Reynolds number Re_p for various values of bed porosities and flow behavior indexes. An expression for the product ($f\ Re_p$) in terms of the porosity and flow behavior index is developed which well predicts experimental values of friction factor for power law flow through packed and fluidized beds.

V. Mohan is with the Department of Chemical Engineering, Illinois Institute of Technology, Chicago, Illinois 60616. J. Raghuraman is with the Department of Chemical Engineering, Monash University, Clayton, Victoria 3168, Australia.